JOURNAL OF CATALYSIS 148, 323–333 (1994)

Partial Oxidation of Methane to Carbon Monoxide and Hydrogen with Molecular Oxygen and Nitrous Oxide over Hydroxyapatite Catalysts

Yasuyuki Matsumura* and John B. Moffat[1]

*Department of Chemistry and Guelph–Waterloo Centre for Graduate Work in Chemistry, University of Waterloo, Waterloo, Ontario, N2L 3G1, Canada; and *Osaka National Research Institute, AIST, Midorigaoka, Ikeda, Osaka 563, Japan*

Received August 9, 1993; revised February 22, 1994

Hydroxyapatites catalyze the partial oxidation of methane to carbon monoxide and hydrogen with molecular oxygen at a reaction temperature as low as 600°C. The predominant reactions can be stoichiometrically represented as $CH_4 + O_2 \rightarrow CO_2 + 2H_2$ and $CH_4 + O_2 \rightarrow CO + H_2 + H_2O$. The former reaction is mainly catalyzed over stoichiometric apatite and the latter proceeds over the nonstoichiometric form. With oxygen as oxidant the H_2/CO_x ratios produced are strongly dependent on the Ca/P ratio in the hydroxyapatite, while with nitrous oxide little or no hydrogen is formed. With nitrous oxide as oxidant the active species on the hydroxyapatite are apparently capable of extracting hydrogen from methane, while in the presence of oxygen the active sites appear to interact directly with the carbon atoms. Rate data and infrared spectra of the apatite samples suggest that new sites, which are formed from $P_2O_7^{4-}$ present in nonstoichiometric apatite, are responsible for the selective formation of carbon monoxide.

INTRODUCTION

Hydroxyapatites, generally expressed as $Ca_{10-z}(HPO_4)_z(PO_4)_{6-z}(OH)_{2-z}$ ($0 \leq z \leq 1$), often function as acid–base catalysts (1–7). The solid synthesized by precipitation in a solution containing calcium and phosphate ions is microcrystalline and usually has a relatively high surface area (8). Since calcium ions in hydroxyapatite can be ion-exchanged with other divalent cations (9, 10), implantation of catalytically active metal ions on apatite is possible. For example, the apatite ion-exchanged with lead is an effective catalyst for the oxidative coupling of methane to ethane and ethylene at a reaction temperature as low as 700°C, while hydroxyapatite itself catalyzes methane oxidation mainly to carbon oxides at 700°C (11, 12). Although the lead ions on the surface of apatite apparently play an important role in the activation of methane, the activation sites for oxygen on lead-modified and unmodified apatites appear to be similar (12). While a variety of oxygen species, O^-, O^{2-}, O_2^-, and O_2^{2-}, as well as F-centers (13), have been proposed as intermediate species for methane coupling (14, 15), direct detection of such species under reaction conditions is difficult.

It is known that the partial oxidation of methane to methanol, formaldehyde, or carbon monoxide can proceed at a lower temperature than the coupling (16), while at the higher temperatures employed in the latter process the formation of partial oxidation products is not favored. Formaldehyde and methanol are produced over molybdenum or vanadium oxide catalysts with either nitrous oxide or oxygen (17–24), although the yields have generally been found to be higher with the former oxidant. However, recent work with molybdenum oxide supported on silica has shown that both the conversion of methane and the selectivity to formaldehyde are higher with oxygen than with nitrous oxide (25). Various sites have been proposed as active in this process (16, 22), including O-species and oxygen vacancies. In contrast, formaldehyde can be produced over silica with dioxygen, although the catalyst does not yield formaldehyde with nitrous oxide (26). These results suggest that dioxygen or species generated from dioxygen are also able to participate in the partial oxidation of methane. Thus, the partial oxidation should take place at relatively low temperatures over hydroxyapatite if such oxygen species, which can activate methane, are generated on the surface from dioxygen.

Since hydroxyapatites with different Ca/P ratios often display dissimilar behavior in catalytic reactions, it is anticipated that the catalytic activity of this solid in the partial oxidation of methane will also show dependencies on the elemental composition. Hence, studies of the oxidation of methane on hydroxyapatites can provide information on the properties of the solid and how these vary with composition, as well as on the oxidation process and the structural features of the active sites for the partial oxidation of methane with dioxygen.

[1] To whom correspondence should be addressed.

0021-9517/94 $6.00

In the present work, the results of reaction studies will be employed to show that the activities and selectivities exhibited by hydroxyapatite in the oxidation of methane are dependent both on the elemental composition of the catalyst and on the oxidant employed. Reaction studies with oxygen and nitrous oxide and hydroxyapatite samples of various Ca/P ratios, together with infrared spectroscopy, are used to provide information on the structural features of the catalyst, the reaction mechanism, and the nature of the active sites.

EXPERIMENTAL

Hydroxyapatites ($Ap_{1.65}$, $Ap_{1.63}$, $Ap_{1.61}$, $Ap_{1.55}$, and $Ap_{1.51}$, where the subscripts represent the Ca/P molar ratio of the apatities) were prepared from $Ca(NO_3)_2 \cdot 4H_2O$ (BDH AnalaR) and $(NH_4)_2HPO_4$ (BDH AnalaR) according to the method described in Ref. (27). The resulting solids were usually heated in air at 500°C for 3 h after drying at 120°C for 18 h; then they were powdered to 180–300 mesh. The Ca/P molar ratio of the prepared hydroxyapatite was determined by analyzing the concentrations of Ca^{2+} and PO_4^{3-} ions in the solution remaining from the synthesis by ion chromatography (Dionex 4500i). Formation of hydroxyapatite was confirmed by recording the X-ray diffraction (XRD) patterns for these samples (28). The sample of β-calcium pyrophosphate ($Ca_2P_2O_7$) was prepared by heating $CaHPO_4$ (BDH) in air at 860°C for 3 h (3) and β-tricalcium phosphate ($Ca_3(PO_4)_2$) was obtained by heating $Ap_{1.51}$ at 1000°C for 2 h (11, 29). Calcium carbonate ($CaCO_3$, BDH AnalaR) was heated in air at 500°C.

Methane conversion was performed in a conventional fixed-bed continuous flow reactor operated under atmospheric pressure. The reactor consisted of a quartz tube of 9 mm i.d. and 35 mm length sealed at each end to a 4 mm i.d. quartz tube. The reaction temperature was measured with a thermocouple located on the reactor wall. The catalyst was sandwiched with quartz wool plugs, whose contribution to the reaction was negligible. No solid diluent of the catalyst was used. The reactants (CH_4, 9–29 kPa; O_2 or N_2O, 2–15 kPa) were diluted with helium gas and the total flow rate was 0.9 $dm^3\ h^{-1}$ (S.T.P.). In a number of reactions water was fed to the reactant stream with a separate flow of helium leading from a water saturator at room temperature (H_2O, 2 kPa if present, total flow rate 0.9 $dm^3\ h^{-1}$). Apatite catalysts (0.15–1.50 g) were preheated in the flow of oxygen diluted with helium (O_2, 6 kPa; total flow rate, 0.6 $dm^3\ h^{-1}$) at 600°C for 1 h. The reactants and products were analyzed with an on-stream gas chromatograph (HP5880) equipped with a TCD. Two columns, one a Porapak T (5.4 m) or HayeSep Dip (5.4 m), the other a Molecular Sieve 5A (0.4 m), were employed in the analyses. The composition of the reaction gas was determined by using calibration curves for all of the reactants and products detected except water. In the concentration ranges required in the present work the calibration curve for formaldehyde was linear but that for hydrogen was slightly nonlinear. Selectivities (mol%) were calculated on the basis of the carbon contents in products determined by the GC analysis. Carbon and oxygen balances were always better than 97% throughout each reaction. The quantity of hydrogen molecules detected corresponded stoichiometrically to the quantities of the products and oxygen consumed. The measurements were reproducible even with different quantities of the catalysts at the same space velocity, suggesting that the reaction is not controlled by diffusion of gas in the reactor.

The surface areas of the catalysts were measured by the conventional BET nitrogen adsorption method.

Infrared (IR) spectra were recorded with a Bomem MB-100 FTIR. The sample (0.03 g) was pressed into a self supporting wafer and mounted in an IR cell constructed from KBr windows and a quartz tube, permitting heating under vacuum. The sample was heated *in vacuo* at 600°C for 1 h before the measurement of the spectra at room temperature (spectral range, 400–5500 cm^{-1}; resolution, 4 cm^{-1}; number of scans, 20). After adsorption of carbon dioxide or pyridine on the sample at 100°C, the sample was evacuated at the desired temperature and its IR spectrum was recorded.

RESULTS

Partial Oxidation of Methane with Dioxygen on Hydroxyapatite Catalysts

Hydroxyapatites effectively catalyzed the partial oxidation of methane with dioxygen at 600°C (Fig. 1 and Table 2). Products detected were carbon monoxide, carbon dioxide, formaldehyde, hydrogen, and water. Although hydroxyapatite of approximately stoichiometric composition ($Ap_{1.65}$) mainly produced carbon dioxide, the molar ratio of H_2/CO_x in the products was as high as 1.3. The selectivity to carbon monoxide increased with decrease in the Ca/P ratio of hydroxyapatite down to 1.61, while the ratio of H_2/CO_x decreased with decrease in the Ca/P ratio. In separate experiments water was intentionally added to the reactant stream and the partial oxidation of methane was carried out over 0.30 g of $Ap_{1.65}$ and $Ap_{1.61}$. No significant changes in the product distribution were observed in comparison with the corresponding reactions without water shown in Table 2. The BET surface areas of the catalysts after 3 h on-stream are shown in Table 1.

In order to compare the activities per unit surface area of $Ap_{1.65}$ and $Ap_{1.61}$, the rates of conversion of methane

TABLE 1

BET Surface Area of Hydroxyapatite Samples

Sample	Surface area/$m^2\ g^{-1}$		
		After reaction[a]	
	As prepared	with O_2	with N_2O
$Ap_{1.65}$	53.6	41.5	38.8
$Ap_{1.63}$	54.8	43.4	39.1
$Ap_{1.61}$	57.9	37.5	46.0
$Ap_{1.55}$	61.7	42.5	49.8
$Ap_{1.51}$	71.7	50.4	53.4

[a] The samples were obtained after reactions illustrated in Figs. 1 and 5.

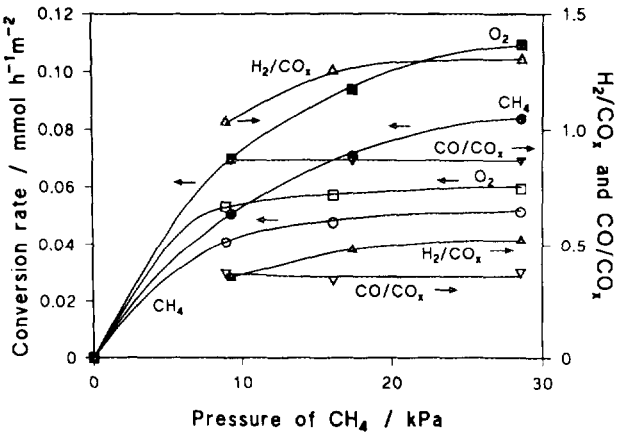

FIG. 2. Dependence of conversion rate of methane and dioxygen on the partial pressure of methane. Open symbols, $Ap_{1.65}$: solid symbols, $Ap_{1.61}$: reaction conditions; catalysts, 0.30 g; partial pressure of dioxygen, 9 kPa; total flow of reactant gas, 0.9 $dm^3\ h^{-1}$; reaction temperature, 600°C; time on stream, 3 h.

and of oxygen were calculated after 3 h on-stream from the surface areas of the catalysts subsequent to the 3 h reaction. As shown in Fig. 2, the conversion rates of methane and dioxygen for $Ap_{1.61}$ (solid symbols) were higher than those for $Ap_{1.65}$ (open symbols) and the H_2/CO_x ratio increased with the partial pressure of methane with both catalysts, while the CO/CO_x ratio remained constant for pressures of methane from 10 to 30 kPa. The conversion rates increased with the partial pressure of methane but with $Ap_{1.65}$ the change in conversion rates with the partial pressure of methane became relatively small for pressures of 8 kPa or larger.

With increase in the pressure of oxygen the rates of conversion of methane and of oxygen increased rapidly with both catalysts, only beginning to approach a plateau for pressures of oxygen greater than 8 kPa and with the $Ap_{1.61}$ catalyst (Fig. 3). As noted in Fig. 3, the rates for the $Ap_{1.61}$ catalyst were greater than those for the $Ap_{1.65}$ catalyst at all pressures of oxygen. The ratio CO/CO_x was virtually constant for both catalysts with increase in the pressure of oxygen while the ratio H_2/CO_x decreased.

An appreciable quantity of formaldehyde was formed over $Ap_{1.55}$ and $Ap_{1.51}$. It is noteworthy that the selectivities changed relatively little with change in the quantity of $Ap_{1.65}$ or $Ap_{1.61}$ held in the reactor under the experimental conditions, while the ratio of H_2/CO_x discernibly decreased with increase in the mass of the catalysts em-

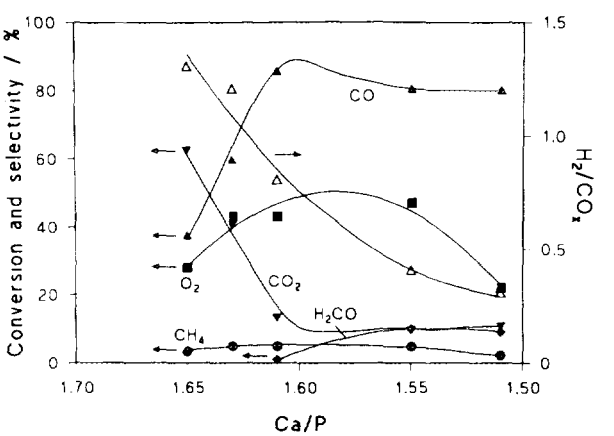

FIG. 1. Partial oxidation of methane with dioxygen over hydroxyapatites of various Ca/P ratios. Reaction conditions; catalysts, 0.30 g; partial pressure of methane, 29 kPa; dioxygen, 4 kPa; total flow of reactant gas, 0.9 $dm^3\ h^{-1}$; reaction temperature, 600°C; time on stream, 3 h.

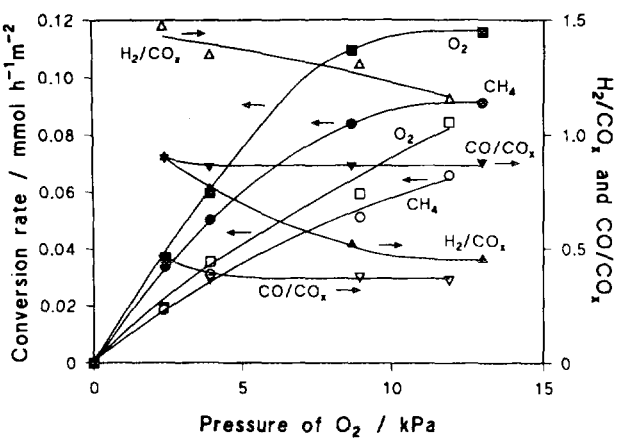

FIG. 3. Dependence of conversion rate of methane and oxygen on the partial pressure of dioxygen. Open symbols, $Ap_{1.65}$: solid symbols, $Ap_{1.61}$: reaction conditions; catalysts, 0.30 g; partial pressure of methane, 29 kPa; total flow of reactant gas, 0.9 $dm^3\ h^{-1}$; reaction temperature 600°C; time on stream, 3 h.

TABLE 2

Partial Oxidation of Methane with Dioxygen over Hydroxyapatites[a]

Catalyst	Amount/g	Conversion/%		Selectivity/%			
		CH_4	O_2	H_2CO	CO	CO_2	H_2/CO_x^b
$Ap_{1.65}$	0.60	5.5	46	0.0	38.2	61.8	1.3
$Ap_{1.65}$	0.30	3.4	28	0.0	37.2	62.8	1.3
$Ap_{1.61}$	0.60	7.2	61	0.7	87.1	12.2	0.7
$Ap_{1.61}$	0.30	5.0	43	1.1	85.3	13.6	0.8
$Ap_{1.61}$	0.15	2.6	22	1.1	88.6	10.3	0.8
$Ap_{1.51}$	0.60	4.1	40	4.5	68.6	26.9	0.3
$Ap_{1.51}$	0.30	2.3	22	9.1	79.8	11.1	0.3
$Ap_{1.61}^c$	0.60	0.6	6	2.9	70.3	26.8	0.8

[a] Reaction conditions unless otherwise mentioned: partial pressure of methane, 29 kPa; dioxygen, 4 kPa; total flow of reactant gas, 0.9 $dm^3\ h^{-1}$; reaction temperature, 600°C; time on stream, 3 h.

[b] Molar ratio of $H_2/(CO + CO_2)$ in product gas.

[c] Reaction temperature, 500°C.

ployed. Over $Ap_{1.51}$ the selectivity to carbon dioxide increased by a factor of 2, with a corresponding increase in the mass of the catalyst contained in the reactor (see Table 2). No peaks other than those attributed to hydroxyapatite were present in the XRD patterns for the apatite catalysts removed from the reactor after the reaction (28). Since the crystalline structure of hydroxyapatites with a Ca/P molar ratio close to 1.50 is partially converted to that of β-tricalcium phosphate by heating at 700°C or above (11), the XRD results suggest no significant formation of hot spots in the catalyst layer. The white color of the catalysts remained unchanged after the reaction.

At a reaction temperature of 500°C the conversions were low; however, the selectivity to carbon monoxide was 70.8% with 0.60 g of $Ap_{1.61}$ and the molar ratio of H_2/CO_x in the products was 0.8, showing that the partial oxidation of methane over hydroxyapatite is possible at temperatures as low as 500°C (Table 2).

The conversions of methane and dioxygen gradually decreased with time on stream during the partial oxidation of methane over the hydroxyapatite catalysts. For example, 0.30 g of $Ap_{1.65}$ produced methane conversions of 3.8 and 3.4% after 0.5 h and 3 h on stream, respectively, while the product distribution did not change significantly (not shown). On the other hand, over 0.30 g of $Ap_{1.61}$ the selectivity to carbon monoxide increased by a small but discernible amount from 84.6 to 85.3% after 0.5 h and 3 h on-stream, respectively, while the methane conversion decreased from 5.3 to 5.0%, respectively (not shown). A similar tendency was observed in other reactions with dioxygen at 600°C over $Ap_{1.61}$. No significant change in product distribution was observed with other nonstoichiometric apatite catalysts.

In order to provide additional evidence for this phenomenon, the reaction over $Ap_{1.61}$ was carried out for an extended period of time. The conversions of methane and dioxygen decreased appreciably during the initial stages of the reaction over 1.50 g of $Ap_{1.61}$ (Fig. 4). Initially, the conversions of methane and dioxygen were more than 20 and 80%, respectively. The selectivity to carbon monoxide was 76.8% after 0.5 h on stream and increased to 85.9% after 48.0 h on stream, while the H_2/CO_x ratio decreased from 0.6 to 0.5. The formation of a small amount of formaldehyde was observed after 24.0 h on stream. The surface area of $Ap_{1.61}$ after 48 h on stream was 27.0 $m^2\ g^{-1}$ in comparison with 48.7 $m^2\ g^{-1}$ and 48.2 $m^2\ g^{-1}$ obtained immediately after pretreatment, the latter

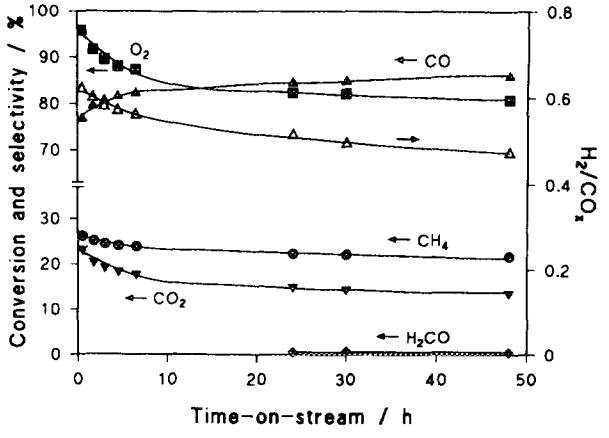

FIG. 4. Partial methane oxidation with dioxygen over $Ap_{1.61}$. Reaction conditions: catalyst, 1.50 g; partial pressure of methane, 29 kPa; partial pressure of oxygen, 10 kPa; total flow of reactant gas, 0.9 $dm^3\ h^{-1}$; reaction temperature 600°C.

TABLE 3

Oxidation of Methane with Nitrous Oxide over Hydroxyapatites[a]

Catalyst	Amount/g	Conversion/%		Selectivity/%			
		CH_4	N_2O	C_2H_6	C_2H_4	CO	CO_2
$Ap_{1.65}$	0.60	2.6	37	1.9	2.6	13.1	82.3
$Ap_{1.65}$	0.30	1.6	23	2.9	1.2	14.3	81.6
$Ap_{1.61}$	0.60	1.3	18	1.9	0.2	24.7	73.3
$Ap_{1.61}$	0.30	0.7	10	2.6	0.0	23.4	74.0
$Ap_{1.51}$	0.60	0.5	6	2.0	0.2	41.8	55.9
$Ap_{1.51}$	0.30	0.3	4	3.4	0.1	38.0	58.5

[a] Reaction conditions unless otherwise mentioned: partial pressure of methane, 29 kPa; nitrous oxide, 7 kPa; total flow of reactant gas, 0.9 $dm^3\ h^{-1}$; reaction temperature, 600°C; time on stream, 3 h.

for $Ap_{1.65}$. No peaks attributed to other than hydroxyapatite appeared in the XRD pattern for the catalyst after the reaction (28).

Partial Oxidation of Methane with Nitrous Oxide on Hydroxyapatite Catalysts

Methane oxidation was carried out with nitrous oxide over hydroxyapatites. The conversions of methane and nitrous oxide decreased with decrease in the Ca/P ratio of the samples, while selectivity to carbon monoxide increased (Fig. 5 and Table 3). The selectivity to carbon monoxide with nitrous oxide was smaller than that found with dioxygen, and carbon dioxide was a major product. Small amounts of ethane and ethylene were detected. The values of the surface area for these catalysts after 3 h on stream are shown in Table 1. The selectivities to carbon oxides were similar when the conversions of the reactants were increased by increases in the quantity of catalyst in the reactor (see Table 3). A discernible amount of hydrogen was formed in the run with 0.60 g of $Ap_{1.65}$ (the H_2/CO_x molar ratio was 0.18), while the quantity of hydrogen produced was very small with 0.30 g of $Ap_{1.65}$. No formation of hydrogen was detected in the reactions with the remaining apatite catalysts shown in Table 3. The color of the catalysts was found to be black after the reaction, indicating the formation of coke during the reaction, although with dioxygen no evidence for coke formation was found.

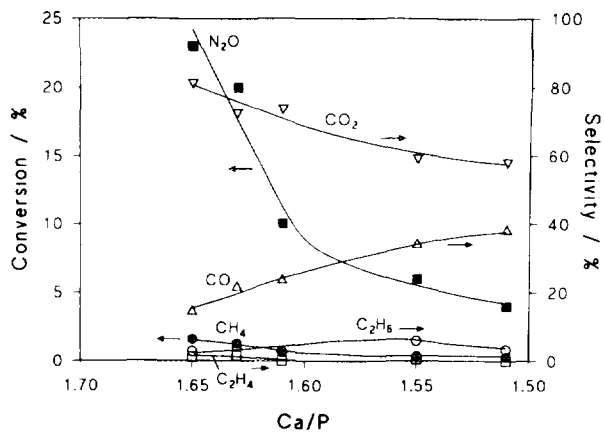

FIG. 5. Oxidation of methane with nitrous oxide over hydroxyapatite. Reaction conditions; catalysts, 0.30 g; partial pressure of methane, 29 kPa; nitrous oxide, 7 kPa; total flow of reactant gas, 0.9 $dm^3\ h^{-1}$; reaction temperature, 600°C; time on stream, 3 h.

Decomposition of nitrous oxide to nitrogen and dioxygen is a thermodynamically favorable reaction at 600°C (ΔG of the reaction $2N_2O \rightarrow 2N_2 + O_2$ at 600°C is calculated as -295 kJ mol^{-1}). Although dinitrogen and dioxygen were not separated in the GC analysis, the amount of nitrous oxide consumed in the reaction with methane corresponded to the amount of nitrogen formed, as determined by assuming that no dioxygen was formed in the reaction; that is, the conversion of nitrous oxide was almost the same as the yield of dinitrogen calculated according to the assumption. Hence, the amount of dioxygen in the product gas is negligible. In the case of the reaction where methane was not fed (catalyst, 0.30 g; partial pressure of nitrous oxide, 7 kPa; total flow of reactant gas, 0.9 $dm^3\ h^{-1}$; reaction temperature, 600°C; time on stream, 0.5 h), dioxygen was produced over the apatite catalysts. The values for the conversion of nitrous oxide in the absence of methane were 7.4% for $Ap_{1.65}$, 5.6% for $Ap_{1.63}$, 4.5% for $Ap_{1.61}$, 3.4% for $Ap_{1.55}$, and 2.3% for $Ap_{1.51}$.

Methane Oxidation with Dioxygen and Nitrous Oxide on Calcium Compounds

It has been reported that $P_2O_7^{4-}$ and CO_3^{2-} groups are present in the structure of hydroxyapatite, in which PO_4^{3-} is a major anion species (5, 29–31). In order to estimate

TABLE 4

Methane Oxidation over Calcium Compounds[a]

Catalyst	Oxidant[b]	Conversion		Selectivity					
		CH_4	O_2 or N_2O	C_2H_6	C_2H_4	H_2CO	CO	CO_2	H_2/CO_x[c]
$Ca_2P_2O_7$	O_2 (2.9)	0.1	0.7	0.0	0.0	19.3	12.6	68.1	0.0
$CaCO_3$	O_2 (3.3)	0.8	3	0.0	0.0	0.0	33.6	66.4	1.1
$Ca_3(PO_4)_2$	O_2 (3.0)	2.8	9	0.0	0.0	0.0	56.0	44.0	1.2
$Ap_{1.65}$[d]	O_2 (3.2)	5.6	21	0.0	0.0	0.0	38.1	61.9	1.3
$Ca_2P_2O_7$	N_2O (2.0)	0.1	0.4	49.7	4.8	0.0	21.4	24.1	0.0
$CaCO_3$	N_2O (1.9)	0.7	5	19.9	0.0	0.0	6.3	73.7	tr[e]
$Ca_3(PO_4)_2$	N_2O (2.0)	1.1	7	9.1	0.7	0.0	21.6	68.6	0.0
$Ap_{1.65}$[d]	N_2O (2.0)	1.6	12	3.1	0.2	0.0	18.7	77.9	0.0

[a] Reaction conditions unless otherwise mentioned: catalyst, 0.60 g; partial pressure of methane, 29 kPa; total flow of reactant gas, 0.9 $dm^3\ h^{-1}$; reaction temperature, 600°C; time on stream, 3 h.

[b] (molar ratio of CH_4/oxidant in feedstream).

[c] Molar ratio of $H_2(CO + CO_2)$ in product gas.

[d] Amount of catalyst, 0.30 g.

[e] Trace amount of hydrogen was detected.

the contributions of these groups to the catalytic process, methane oxidation with dioxygen and with nitrous oxide was carried out over $Ca_2P_2O_7$, $CaCO_3$, and $Ca_3(PO_4)_2$ (Table 4). With dioxygen as the oxidant $Ca_2P_2O_7$ produced high selectivities (≈19.3%) to formaldehyde, while no hydrogen was detected. The major product with these catalysts was carbon dioxide and the conversions of the reactants were very low. Although $CaCO_3$ also produced low conversions of methane and dioxygen, the product distribution was similar to that of $Ap_{1.65}$. With oxygen over $Ca_3(PO_4)_2$ hydrogen was formed as well as with $CaCO_3$ while the conversions and the selectivities to carbon monoxide were higher with the former than the latter. The values of the surface areas of these catalysts measured after 3 h on stream were 0.4 $m^2\ g^{-1}$ for $Ca_2P_2O_7$, less than 0.3 $m^2\ g^{-1}$ for $CaCO_3$, and 3.7 $m^2\ g^{-1}$ for $Ca_3(PO_4)_2$.

When the oxidant was nitrous oxide, $Ca_2P_2O_7$ produced significantly high selectivities to C_2 compounds while the conversions were low. Carbon dioxide was a principal product in the reaction over $CaCO_3$ and a very small quantity of hydrogen was detected. No formation of hydrogen was observed in the reactions with $Ca_2P_2O_7$ and $Ca_3(PO_4)_2$ in the presence of nitrous oxide.

Characterization of Hydroxyapatite by Infrared Spectroscopy

Although no peaks attributed to calcium carbonate were present in the XRD patterns of the hydroxyapatite samples, IR absorption bands attributed to CO_3^{2-} were observed at 1379, 1412, and 1454 cm^{-1} (Fig. 6a) (5). The intensity of the bands decreased with decrease in the Ca/P molar ratio of the apatite samples (circles in Fig. 7) as reported by Bett *et al.* (5), while similar shapes of the peaks were recorded regardless of the samples. The intensity of the band at 3571 cm^{-1} assigned to the stretching vibration of OH^- groups also decreased with decrease in the Ca/P molar ratio (squares in Fig. 7) (31). Bands attributed to $P_2O_7^{4-}$ were observed at 727 cm^{-1} in the IR spectra of $Ap_{1.61-1.51}$ (Fig. 8) (29, 30). The band at 878 cm^{-1} assignable to the symmetrical stretching vibration of P–O(H) groups in HPO_4^{2-} was observed in the spectra of $Ap_{1.65-1.61}$ (29–31). It is noteworthy that $Ap_{1.65}$ provided the strongest intensity of the band at 878 cm^{-1}, although the num-

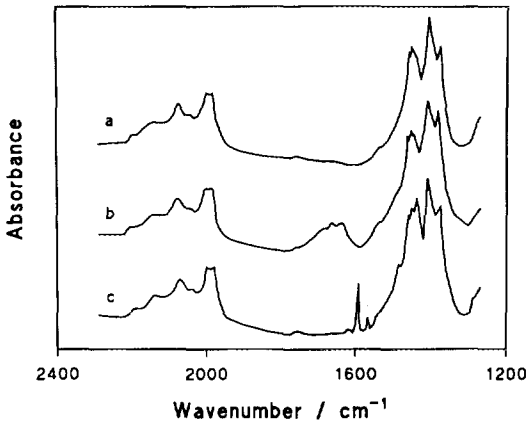

FIG. 6. IR spectra of $Ap_{1.65}$ (a) evacuated at 600°C for 1 h, (b) after adsorption of carbon dioxide followed by evacuation at room temperature for 1 h, (c) after adsorption of pyridine followed by evacuation at 100°C for 1 h.

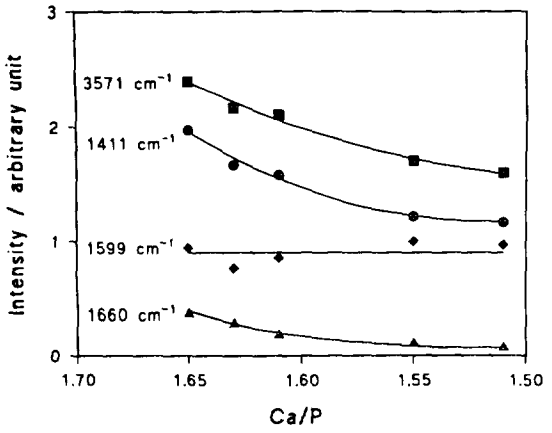

FIG. 7. Peak intensities for the IR absorption bands at 1599, 1660, 3571, and 1412 cm^{-1} attributed to adsorbed pyridine, adsorbed carbon dioxide, OH^- and CO_3^{2-}, respectively. The abscissa shows the Ca/P molar ratio of hydroxyapatites. The peak intensities are normalized with the absorption band at 1998 cm^{-1} assigned to the PO_4^{3-} harmonic.

ber of HPO_4^{2-} groups in $Ap_{1.65}$ calculated from the stoichiometry of apatite is the smallest in the apatite samples. Although a strong band was observed at 727 cm^{-1} in the spectrum for $Ap_{1.61}$, which had been evacuated at 200°C for 1 h after drying at 120°C, the band at 878 cm^{-1} was as weak as that in the spectrum of $Ap_{1.61}$ evacuated at 600°C (Fig. 8). The IR band at 727 cm^{-1} was not observed in the spectrum for $Ap_{1.61}$ removed from the reactor after the reaction shown in Fig. 4 while the intensity of the band at 878 cm^{-1} was similar to that for $Ap_{1.61}$ just after the pre-

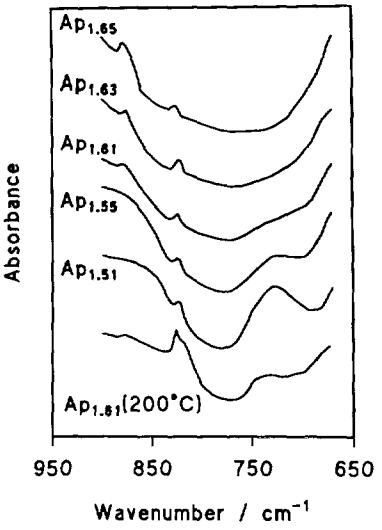

FIG. 8. IR spectra of hydroxyapatites evacuated at 600°C for 1 h. The bottom spectrum is that for $Ap_{1.61}$ evacuated at 200°C for 1 h after drying at 120°C for 18 h.

treatment. The assignment of the band at 828 cm^{-1} is not clear, but it may be attributed to the basic structure of hydroxyapatite because the band can be observed regardless of the Ca/P molar ratio in the samples.

New absorption bands appeared at 1600–1700 cm^{-1} after adsorption of carbon dioxide on the apatite samples followed by evacuation at room temperature for 1 h (Fig. 6b). Since the wave number of the bands is close to that of the band observed in adsorption of carbon dioxide on zinc oxide (1640 cm^{-1}), the bands can be attributed to an adsorption species of carbon dioxide on the surface, possibly carbon dioxide interacting with surface oxygen but different in structure from the CO_3^{2-} ion (32). No increment in the bands at 1300–1550 cm^{-1} was observed after adsorption of carbon dioxide. The intensity of the band at ca. 1660 cm^{-1} decreased with decrease in the Ca/P ratio of the samples (triangles in Fig. 7). The intensity of the band at 878 cm^{-1} decreased appreciably after the adsorption of carbon dioxide, while no significant change in the intensity of the band at 3571 cm^{-1} was observed (not shown). The band at 878 cm^{-1} was almost eliminated after evacuation at 100°C for 1 h and vanished after evacuation at 200°C for 1 h (not shown). On the other hand, new bands at 1444, 1489, 1575, and 1599 cm^{-1} appeared after adsorption of pyridine on the apatite samples followed by evacuation at 100°C for 1 h, while the bands at 1444 and 1489 cm^{-1} overlapped the bands attributed to CO_3^{2-} at 1300–1550 cm^{-1} (Fig. 6c). Those bands are generally attributed to physisorbed pyridine (33). The intensity of the band at 1599 cm^{-1} did not vary significantly with changes in the Ca/P ratio of the samples (diamonds in Fig. 7). The intensity of the band decreased considerably after evacuation at 200°C for 1 h (not shown).

The peak intensities shown in Fig. 7 were normalized with the absorption band at 1998 cm^{-1} assigned to the PO_4^{3-} harmonic (31). The intensity was evaluated on the basis of the peak heights of the bands.

DISCUSSION

Mechanism of Methane Oxidation

Although a considerable quantity of dioxygen is produced from nitrous oxide over hydroxyapatites in the absence of methane, the formation of dioxygen cannot be confirmed in the oxidation of methane with nitrous oxide. The conversion of nitrous oxide in the presence of methane is higher than that in the absence of methane, suggesting that decomposition of nitrous oxide is enhanced by the presence of methane. Hence, it appears that the decomposition of nitrous oxide to form dioxygen and nitrogen is inhibited by the presence of methane. The catalytic activity of hydroxyapatite in the oxidation of methane with nitrous oxide decreases with decrease in the

Ca/P ratio of the solid and the same tendency was observed in the reaction with nitrous oxide in the absence of methane, suggesting that the active sites for nitrous oxide are similar in both reactions.

Nitrous oxide is known to produce O^- species over some inorganic solids (34, 35). Since O^- species are very reactive, they can extract hydrogen atoms from methane (35). The reactivity of O^- with methane is significantly higher than with hydrogen (35), suggesting that O^- reacts readily with methane. The selectivity to carbon monoxide is low in methane oxidation over hydroxyapatites with nitrous oxide, while a small quantity of C_2 compounds (selectivities ≈2–4%) is formed with nitrous oxide. It is generally believed that the formation of C_2 compounds is due to the coupling of CH_3 radicals (14, 15, 36). Over $Ap_{1.65}$ a discernible amount of hydrogen was observed at the higher conversions produced with 0.60 g of the catalyst in the methane oxidation with nitrous oxide, while 0.30 g of the solid yields a trace amount of hydrogen, suggesting that hydrogen is produced in a subsequent reaction such as the conversion of ethane to ethylene. This is consistent with the observation that the quantities of hydrogen formed in the reactions at low conversions over other apatite catalysts are very small. Hence, it appears that methane reacts with the surface oxygen species without formation of hydrogen; that is, the surface oxygen species actively abstract the hydrogen atoms from methane. Thus, O^- species appear to be the primary oxygen species in the oxidation of methane with nitrous oxide over hydroxyapatite. Coke formation on the catalysts may be due to further abstraction of hydrogen atoms from CH_x on the surface.

Hydroxyapatite produces a significant amount of hydrogen in the oxidation of methane with dioxygen, suggesting that the surface oxygen species are different from those produced from nitrous oxide. The selectivities do not change significantly in the oxidation of methane with dioxygen over different quantities of $AP_{1.65}$ or $Ap_{1.61}$ when the conversions are low. Hence, the subsequent oxidation of the carbon monoxide or hydrogen formed during the reaction is small at the low conversions under the reaction conditions probably because the surface oxygen species are not only reactive to carbon monoxide and hydrogen but also to methane. The methane conversion decreased with increase in the molar ratio of CH_4/O_2 in the feedstream, while the selectivity to carbon monoxide increased as well as the H_2/CO_x ratio (see Figs. 2 and 3). The ratio (R) of O_2/CH_4 for both oxygen and methane consumed in the reaction can be calculated from the conversions of methane (CM) and oxygen (CO) and the ratio (F) of CH_4/O_2 in the feedstream, i.e., $R = CO/(CM \times F)$. When the CH_4/O_2 ratio in the feedstream is 7–8, the consumption ratios of O_2/CH_4 are 1.12 for $Ap_{1.65}$, 1.11 for $Ap_{1.63}$, and 1.18 for $Ap_{1.61}$. The ratio decreases with increases in the CH_4/O_2 ratio in the feedstream; for example, 1.07 for $Ap_{1.65}$ ($CH_4/O_2 = 12.2$ in the feedstream) and 1.09 for $Ap_{1.61}$ ($CH_4/O_2 = 11.9$). Thus, the predominant reactions occurring on these catalysts can be represented stoichiometrically as

$$CH_4 + O_2 \rightarrow CO_2 + 2\ H_2 \quad [1]$$

$$CH_4 + O_2 \rightarrow CO + H_2 + H_2O. \quad [2]$$

Since $Ap_{1.65}$ and $Ap_{1.63}$ can produce H_2CO_x ratios higher than one, part of the methane is transformed to carbon oxides and hydrogen without formation of water in the reaction. Hence, the reaction shown in Eq. [1] can occur on the surface and dioxygen species are suggested as the active oxygen species. The water gas shift reaction ($CO + H_2O \rightarrow CO_2 + H_2$) may take place at the reaction temperature since the value of ΔG at 600°C is -1.8 kJ mol^{-1} (37). However, intentional addition of water to the reactant stream did not affect the oxidation of methane, implying that the water gas shift reaction is negligible at least under the reaction conditions employed.

Over nonstoichiometric apatites the selectivity to carbon monoxide is high, while the H_2/CO_x ratio is lower than that for $Ap_{1.65}$. Thus, the reaction in Eq. [2] will be dominant over $Ap_{1.61}$, with dioxygen species assumed to be the active oxygen species. Since the reaction results in the formation of water, interaction between the hydrogen atom in methane and surface oxygen species must be present. The conversion rates of methane and dioxygen depend on the the partial pressure of dioxygen, but are almost independent of the partial pressure of methane (15–30 kPa) in the feedstream over $Ap_{1.65}$ (Figs. 2 and 3), suggesting that the process of oxygen activation is the rate determining step, while the activated oxygen is reactive to methane. On the other hand, over $Ap_{1.61}$ the conversion rates depend not only on the partial pressure of oxygen but also on that of methane, suggesting that the catalyst activates both methane and oxygen. Since the activation of methane must weaken the bond between the hydrogen and carbon atoms in methane, the hydrogen atom is understood to be easily abstracted by the oxygen species. If the active oxygen is a dioxygen species on the surface of $Ap_{1.61}$, CH_3 and OOH species will presumably be formed after abstraction of a hydrogen atom from methane. Since both species are considered to be relatively unstable, further reaction between these species will proceed and formation of H_xCO species is speculated as an intermediate to hydrogen and carbon monoxide. Decomposition of formaldehyde ($H_2CO \rightarrow H_2 + CO$) is a thermodynamically spontaneous reaction at 600°C ($\Delta G = -96.3$ kJ mol^{-1}), while formation of formaldehyde from methane ($CH_4 + \frac{1}{2}O_2 \rightarrow H_2CO + H_2$) is also favorable at 600°C ($\Delta G = -97.9$ kJ mol^{-1}) (37).

Active Sites for Methane Oxidation

Although there are a number of possible active sites for the oxidation of methane on the hydroxyapatites, the most probable appear to be those related to O^{2-}, OH^-, CO_3^{2-}, PO_4^{3-}, HPO_4^{2-}, and $P_2O_7^{4-}$. In what follows, it is concluded that sites related to or formed from $P_2O_7^{4-}$ are primarily responsible for the catalytic properties of the hydroxyapatites in the methane oxidation process.

Although nonstoichiometric hydroxyapatites often function as acid catalysts (1–4), the IR bands of 1400–1700 cm^{-1} for pyridine adsorbed on the apatite samples preheated at 600°C show the absence of acid sites on the surface. The intensity of the absorption band at 1599 cm^{-1} is considered to be related to the number of physisorption sites for pyridine. Since the intensities for the apatite samples are similar, these sites are believed not to be involved in the methane oxidation.

The intensity of the bands at 1300–1500 cm^{-1} attributed to CO_3^{2-} may be related to the selectivity to carbon dioxide in the methane oxidation with either dioxygen or nitrous oxide and the conversions in the reaction with nitrous oxide. The number of carbonate ions on the surface of the stoichiometric apatite is estimated as 0.0008 mmol m^{-2} by Bett *et al.* (5). The conversion rate of methane for the reaction with dioxygen over $CaCO_3$ is calculated as more than 5 mmol h^{-1} m^{-2} from the data in Table 4 and the surface area after the reaction. Since the rate for the reaction with dioxygen over $Ap_{1.65}$ is only 0.5 mmol h^{-1} m^{-2} on the basis of the results in Table 4, it may be concluded that calcium carbonate has high surface activity. The number of carbonate ions on the surface of $CaCO_3$ is calculated as 0.05 mmol m^{-2} from the density. Hence, the turnover number is more than 100 h^{-1} over $CaCO_3$ if the carbonate ions constitute the active sites. Assuming that this turnover number is applicable to the carbonate ions on $Ap_{1.65}$, which produces similar selectivities to those observed with $CaCO_3$ (see Table 4), the contribution of the carbonate to the methane conversion rate for $Ap_{1.65}$ is estimated as 0.08 mmol h^{-1} m^{-2}. The methane conversion rate for $Ca_3(PO_4)_2$ is calculated as 1 mmol h^{-1} m^{-2} from the data in Table 4. The value is comparable to that for $Ap_{1.65}$. Thus, even if the carbonate ions on the surface of stoichiometric hydroxyapatite are responsible for active sites in the oxidation of methane, while calcium oxide, which may be formed by the decomposition of the carbonate at a high temperature, may also be active in the reaction, the phosphate ions are believed to be the predominant contributors to the oxidation process.

The intensity of the band at 1660 cm^{-1} observed after adsorption of carbon dioxide can depend on the number of adsorption sites for carbon dioxide on the surface. The band almost disappears by evacuation at 100°C, suggesting that the adsorption energy is relatively small. The adsorption sites for carbon dioxide on strontium hydroxyapatite, which has a structure similar to that of calcium hydroxyapatite, are basic hydroxyl groups in strontium-rich apatite (Sr/P molar ratio larger than 1.67) and HPO_4^{2-} groups in the nonstoichiometric form (38). Since the basic hydroxyl groups can irreversibly adsorb carbon dioxide even at 300°C (38), such groups are apparently not present on the samples of calcium hydroxyapatite. In general, Sr–OH is more basic than Ca–OH (39). The adsorption strength of P–OH groups in strontium apatite is fairly weak (38). On the basis of the intensity of the IR band at 878 cm^{-1}, it is estimated that the number of HPO_4^{2-} groups is the largest on $Ap_{1.65}$ in the apatite samples and the number decreases with decrease in the Ca/P ratio of the sample (see Fig. 8). Moreover, it was found that the intensity of the band appreciably decreases after adsorption of carbon dioxide. Thus, the adsorption sites for carbon dioxide on hydroxyapatite can be considered to be primarily hydroxyl groups bonded to phosphorus atoms in HPO_4^{2-} groups. Although $Ap_{1.65}$ is approximately stoichiometric, the molar ratio of Ca/P on the surface was determined as 1.4 by means of XPS (12). This shows that the surface is nonstoichiometric, and thus, a significant number of P–OH groups are available on the surface of $Ap_{1.65}$. Since the intensity of the band at 878 cm^{-1} attributed to HPO_4^{2-} relates to the selectivity to carbon dioxide in the reaction with dioxygen (Fig. 1) and to the conversions for the reaction with nitrous oxide (Fig. 5), the sites formed from HPO_4^{2-} may participate in the reaction.

With $Ap_{1.55}$ and $Ap_{1.51}$, on which a considerable amount of formaldehyde is produced with dioxygen, the H_2/CO_x ratio is significantly lower than observed over $Ap_{1.61}$, while the selectivities to carbon oxides are similar (see Table 2). The IR spectra of these samples clearly show the presence of $P_2O_7^{4-}$ species in the solids. Since the selectivity to formaldehyde is significantly high and hydrogen cannot be detected in the oxidation of methane over $Ca_2P_2O_7$ (see Table 4), the sites constituted with $P_2O_7^{4-}$ ions in hydroxyapatites are believed to catalyze the oxidation of methane to formaldehyde as well as the further oxidation of carbon monoxide and hydrogen.

Although the catalytic activity of hydroxyapatites for the oxidation of methane with nitrous oxide decreases with decrease in the Ca/P ratio in the catalysts, the activity for the oxidation with dioxygen increases with increase in the Ca/P ratio up to 1.61. The stoichiometry of hydroxyapatite, for example, $Ca_{10-z}(HPO_4)_z(PO_4)_{6-z}(OH)_{2-z}$ ($0 \le z \le 1$), suggests that the number of HPO_4^{2-} ions in apatites increases with increase in the Ca/P ratio, but the intensity of the IR band attributed to HPO_4^{2-} groups decreases with increase in the ratio and there is no such band in the spectra for $Ap_{1.55}$ and $Ap_{1.51}$ (see Fig. 8).

It is known that condensation of HPO_4^{2-} to $P_2O_7^{4-}$ ($2HPO_4^{2-} \rightarrow P_2O_7^{4-} + H_2O$) takes place by heating nonstoichiometric hydroxyapatite (30, 31). Assuming that there are no HPO_4^{2-} ions in $Ap_{1.55}$ and $Ap_{1.51}$, that is, the stoichiometry of these samples is expressed as $Ca_{10-z}(P_2O_7)_{z/2}(PO_4)_{6-z}(OH)_{2-z}$, the contents of $P_2O_7^{4-}$ ions are calculated as 0.36 mmol g^{-1} for $Ap^{1.55}$ and 0.49 mmol g^{-1} for $Ap_{1.51}$. As can be seen in Fig. 8, the intensity of the band at 727 cm^{-1} for $Ap_{1.51}$ is almost three times as large as that for $Ap_{1.55}$, suggesting that quantities of both HPO_4^{2-} and $P_2O_7^{4-}$ in $Ap_{1.55}$ are smaller than would be expected from the composition. The reaction $2PO_4^{3-} + H_2O \rightarrow 2OH^- + P_2O_7^{4-}$ may occur in hydroxyapatite on heating (29). Since the reaction accompanies formation of OH^- groups, a significant increase in the number of OH^- groups should be observed. However, the intensity of the band at 3571 cm^{-1} attributed to OH^- decreases with decrease in the Ca/P ratio of the apatite samples and corresponds roughly to the number of OH^- ions calculated from the stoichiometry of hydroxyapatite; for example, 1.9 mmol g^{-1} for $Ap_{1.65}$, 1.8 mmol g^{-1} for $Ap_{1.63}$, 1.7 mmol g^{-1} for $Ap_{1.61}$, 1.3 mmol g^{-1} for $Ap_{1.55}$, and 1.1 mmol g^{-1} for $Ap_{1.51}$. Hence, the contribution of this reaction to the formation of $P_2O_7^{4-}$ is estimated to be small. Moreover, the IR band at 727 cm^{-1} attributed to $P_2O_7^{4-}$ is significantly intense in the spectrum of $Ap_{1.61}$ evacuated at 200°C after the synthesis, suggesting that a considerable quantity of $P_2O_7^{4-}$ groups in $Ap_{1.61}$ disappear by evacuation at 600°C.

It is known that the disappearance of $P_2O_7^{4-}$ takes place when the structure of hydroxyapatite is partially converted into β-tricalcium phosphate as expressed by the reaction $P_2O_7^{4-} + 2OH^- \rightarrow 2PO_4^{3-} + H_2O$ (29); however, the XRD patterns for the apatite samples show no change in the crystalline structure. Thus, new sites should be generated from $P_2O_7^{4-}$ in nonstoichiometric apatites by the pretreatment at 600°C. Disproportionation of the anion to PO_4^{3-} and PO_3^- may occur and the oxygen defect would produce a specific catalytic activity although the PO_3^{2-} radical can be stably observed under ESR measurement conditions (40). As shown in Fig. 4, the selectivity to carbon monoxide in the oxidation with dioxygen over $Ap_{1.61}$ increases with time-on-stream while the IR band attributed to $P_2O_7^{4-}$ groups was not observed on the catalyst after the reaction. Since there is no significant change in the band attributed to HPO_4^{2-} after the reaction, the new sites, if present, are expected to produce high selectivity to carbon monoxide. Thus, it is supposed that the new sites can activate methane.

With $CaCO_3$, $Ca_2P_2O_7$, and $Ca_3(PO_4)_2$, the methane conversions in the oxidation with nitrous oxide over each calcium compound are similar to those in the oxidation with dioxygen (see Table 4). Since the surface of hydroxyapatite has some resemblance to those of these compounds, the conversions with dioxygen should parallel those with nitrous oxide. However, the conversions with dioxygen increase with decrease in the Ca/P ratio of the apatite samples up to 1.61 (Fig. 1), while those with nitrous oxide decrease simply with decrease in the Ca/P ratio (Fig. 5). The numbers of HPO_4^{2-} groups in apatites calculated from the stoichiometry are 0.10 mmol g^{-1} for $Ap_{1.65}$, 0.22 mmol g^{-1} for $Ap_{1.63}$, 0.34 mmol g^{-1} for $Ap_{1.61}$, 0.72 mmol g^{-1} for $Ap_{1.55}$, and 0.99 mmol g^{-1} for $Ap_{1.51}$. The number of the new sites in $Ap_{1.61}$ is assumed to be larger than that for $Ap_{1.63}$, since (1) the intensities of the IR band at 878 cm^{-1} attributed to HPO_4^{2-} for $Ap_{1.61}$ and $Ap_{1.63}$ are smaller than that for $Ap_{1.65}$, for which the calculated number of HPO_4^{2-} is the smallest, and (2) the intensity of the band at 727 cm^{-1} for $Ap_{1.61}$ is weak and the band is not observable on $Ap_{1.63}$. The number of new sites in $Ap_{1.65}$ should be smaller than $Ap_{1.63}$, since the intensity of the band attributed to HPO_4^{2-} for the former is larger than that for the latter. Although the calculated number of HPO_4^{2-} for $Ap_{1.51}$ is the largest, the number of new sites in $Ap_{1.51}$ is estimated to be relatively small because the IR spectrum for the sample shows that a significant number of $P_2O_7^{4-}$ are present in the solid. If the new sites activate methane and the activated methane partly assists activation of dioxygen, the conversions with dioxygen will depend on both numbers of the new sites and the activation sites for dioxygen or nitrous oxide. Since the conversion with dioxygen appears to be related to the number of the new sites in hydroxyapatite, the new sites apparently function as the activation sites of methane and are responsible for the increase in the activity of hydroxyapatite to methane oxidation with dioxygen.

ACKNOWLEDGMENT

The financial support of the Natural Sciences and Engineering Research Council of Canada is gratefully acknowledged.

REFERENCES

1. Kibby, C. L., Lande, S. S., and Hall, W. K., *J. Am. Chem. Soc.* **94,** 214 (1972).
2. Kibby, C. L., and Hall, W. K., *J. Catal.* **29,** 144 (1973).
3. Monma, H., *J. Catal.* **75,** 200 (1982).
4. Izumi, Y., Sato, S., and Urabe, K., *Chem. Lett.* 1649 (1983).
5. Bett, J. A. S., Christner, L. G., and Hall, W. K., *J. Catal.* **13,** 332 (1969).
6. Kibby, C. L., and Hall, W. K., *J. Catal.* **31,** 65 (1973).
7. Imizu, Y., Kadoya, M., and Abe, H., *Chem. Lett.* 415 (1982).
8. Bett, J. A. S., Christner, K. G., and Hall, W. K., *J. Am. Chem. Soc.* **89,** 5335 (1967).
9. Suzuki, T., Hatsushika, T., and Hayakawa, Y., *J. Chem. Soc., Faraday Trans. 1* **77,** 1059 (1981).
10. Suzuki, T., Hatsushika, T., and Miyake, M., *J. Chem. Soc., Faraday Trans. 1* **78,** 3605 (1982).
11. Matsumura, Y. and Moffat, J. B., *Catal. Lett.* **17,** 197 (1993).

12. Matsumura, Y., Sugiyama, S., Hayashi, H., Shigemoto, N., Saitoh, K. and Moffat, J. B. *J. Chem. Soc. Faraday Trans.*, in press.
13. Wu, M.-C., Truong, C. M., Coulter, K., and Goodman, D. W., *J. Am Chem. Soc.* **114,** 7565 (1992).
14. Lee, J. S. and Oyama, S. T., *Catal. Rev. Sci. Eng.* **30,** 249 (1988).
15. Amenomiya, Y., Birss, V. I., Goledzinowski, M., Galuszka, J. and Sanger, A. R., *Catal. Rev. Sci. Eng.* **32,** 163 (1990).
16. Pitchai, R. and Klier, K., *Catal. Rev. Sci. Eng.* **28,** 13 (1986).
17. Parkyns, N. D., *Chem. Brit.* 841 (1990).
18. Liu, H.-F., Liu, R.-S., Liew, K. Y., Johnson, R. E., and Lunsford, J. H., *J. Am. Chem. Soc.* **106,** 4117 (1984).
19. Khan, M. M., and Somorjai, G. A., *J. Catal.* **91,** 263 (1985).
20. Zhen, K. J., Khan, M. M., Mak, C. H., Lewis, K. B., and Somorjai, G. A., *J. Catal.* **94,** 501 (1985).
21. Otsuka, K., and Hatano, M., *J. Catal.* **108,** 252 (1987).
22. Ahmed, S., Kasztelan, S., and Moffat, J. B., *Faraday Discuss. Chem. Soc.* **87,** 23 (1989).
23. Spencer, N. D., and Pereira, C. J., *J. Catal.* **116,** 399 (1989).
24. Firsova, A. A., Vorob'eva, G. A., Bobyshev, A. A., Shanshkin, D. P., Margolis, L. Y., and Krylov, O. V., *Kinet. Katal.* **32,** 395 (1990).
25. Banares, M. A., Fierro, J. L. G., and Moffat, J. B., *J. Catal.* **142,** 406 (1993).
26. Kasztelan, S., and Moffat, J. B., *J. Chem. Soc., Chem. Commun,* 1663 (1987).
27. Hayek, E., and Newesely, H., *Inorg. Synth.* **7,** 63 (1963).
28. "Index (Inorganic) to the Powder Diffraction File" (J. V. Smith, Ed.), ASTM Publication No. PDIS-16i Pa, 1966.
29. Monma, H., Ueno, S., and Kanazawa, T., *J. Chem. Technol. Biotechnol.* **31,** 15 (1981).
30. Cant, N. W., Bett, J. A. S., Wilson, G. R., and Hall, W. K., *Spectrochim. Acta Part A* **27,** 425 (1971).
31. Joris, S. J., and Amberg, C. H., *J. Phys. Chem.* **75,** 3172 (1971).
32. Matsushita, S., and Nakata, T., *J. Chem. Phys.* **36,** 665 (1962).
33. Matsumura, Y., Hashimoto, K., and Yoshida, S., *J. Mol. Catal.* **69,** L19 (1991).
34. Kazansky, V. B., *in* "Proceedings of the Sixth International Congress on Catalysis," Vol. 1, p. 50. The Chemical Society, London, 1976.
35. Che, M., and Tench, A. J., *Adv. Catal.* **31,** 77 (1982).
36. Lunsford, J. H., *Catal. Today* **6,** 235 (1990).
37. Vernon, P. D. F., Green, M. L. H., Cheetham, A. K., and Ashcroft, A. T., *Catal. Today* **13,** 417 (1992).
38. Ishikawa, T., Saito, H., and Kandori, K., *J. Chem. Soc., Faraday Trans.* **88,** 2937 (1992).
39. Stiles, A. B., *Catal. Today* **14,** 269 (1992).
40. Horsfield, A., Jorton, J. R., and Whiffen, D. H., *Mol. Phys.* **4,** 475 (1961).